Journal of the Korean Electrochemical Society
Vol. 23, No. 3, 2020, 57-65
https://doi.org/10.5229/JKES.2020.23.3.57

Research Paper
pISSN 1229-1935
eISSN 2288-9000

표면 피막 형성이 $LiCoO_2$ 양극의 고온 열화에 미치는 영향

성종훈 · 푸아드 하산 · 유현덕*

부산대학교 화학과

(2020년 4월 30일 접수 : 2020년 5월 18일 수정 : 2020년 5월 25일 채택)

Accelerated Formation of Surface Films on the Degradation of $LiCoO_2$ Cathode at High Temperature

Jong Hun Sung, Fuead Hasan, and Hyun Deog Yoo*

Department of Chemistry and Chemical Institute for Functional Materials, Pusan National University, Busan 46241, Korea

(Received April 30, 2020 : Revised May 18, 2020 : Accepted May 25, 2020)

초 록

리튬이온전지의 열적 열화 메커니즘을 이해하는 것은 전지의 안전성을 향상시키기 위한 필수적인 과정이다. 본 논문에서는 대표적인 양극물질의 하나인 리튬코발트산화물($LiCoO_2$, LCO)이 고온에서 작동할 때 형성되는 표면 필름에 의한 전기화학적 성능 열화를 조사하였다. 먼저 25°C와 60°C 각각의 온도에서 사이클 테스트를 진행한 결과, 60°C에서 25°C에 비해 저하된 사이클 수명을 보였다. 이후 처음 5사이클을 25°C, 60°C에서 구동시킨 LCO 양극을 각각 25-LCO, 60-LCO라 명명하였으며, 이후 임피던스 및 출력 특성 분석은 25°C에서 진행하였다. 이때 두 샘플 모두 저속에서의 초기 용량은 비슷함에도 불구하고 60-LCO가 25-LCO에 비해 높은 임피던스와 낮은 출력 특성을 보였다. X-선 광전자분광 (XPS)분석 결과 60-LCO 샘플에서 cathode-electrolyte interphase의 성분 중 하나인 절연성의 수산화 리튬 (LiOH) 성분이 다량 검출되었으며, 이는 고온에서 과도한 표면 필름 형성이 양극의 표면 저항 증가 및 속도/수명 특성 저하를 가져왔음을 보여준다.

Abstract : It is crucial to investigate the thermal degradation of lithium-ion batteries (LIBs) to understand the possible malfunction at high temperature. Herein, we investigated the effects of surface film formation on the thermal degradation of lithium cobalt oxide ($LiCoO_2$, LCO) cathode that is one of representative cathode materials. Cycling test at 60°C exhibited poorer cycleability compared with the cycling at 25°C. Cathodes after the initial 5 cycles at 60°C (60-LCO) exhibited higher impedance compared to the cathode after initial 5 cycles at 25°C (25-LCO), resulting in the lower rate capability upon subsequent cycling at 25°C, although the capacity values were similar at the lowest C-rate of 0.1C. In order to understand degradation of the LCO cathode at the high temperature, we analyzed the cathodes surface using X-ray photoelectron spectroscopy (XPS). Among various peaks, intensity of lithium hydroxide (LiOH) increased substantially after the operation at 60°C, and the C-C signal that represents the conductive agent was distinctly lower on 60-LCO compared to 25-LCO. These results pointed to an excessive formation of cathode-electrolyte interphase including LiOH at 60°C, leading to the increase in the resistance and the resultant degradation in the electrochemical performances.

Keywords : Lithium Cobalt Oxide, Surface Film, Thermal Degradation, Lithium-Ion Batteries, Resistance

*E-mail: hyundeog.yoo@pusan.ac.kr

1. Introduction

Lithium ion batteries (LIBs) have been widely used, owing to high energy density and long cycle life.[1-6] Recently, utilization of LIBs has been extended to the electric vehicles (EVs) or energy storage systems (ESSs) as well as portable electronic devices.[7,8] Such larger-scale LIBs for EVs or ESSs have to gratify much more stringent requirements, such as higher energy density, safety, and wider range of temperature for the operation.[9,10] Especially, the safety has become the first and foremost requirements in the use of LIBs in addition to the electrochemical performances.[11] If cycled inappropriately, the chemical energy in LIBs can be released in the form of explosion.[12-14] The fire accidents or explosions that are related with LIBs are reported worldwide these days, particularly with larger scale application such as EVs and ESSs.[15] One of the key factors is the resistance of the LIBs; the increase in the resistance results in more pronounced Joule heating, which accelerates the increase in the resistance and corresponding overheating over and over again, which lead to serious instability of LIBs at the end. These serious problems call for the continued research on the degradation of LIBs in extraordinary conditions such as high temperature, overcharging, and high voltage operation.

Lithium cobalt oxide ($LiCoO_2$, LCO), which is a layered cathode for LIBs, has a high theoretical capacity and energy density.[16] However, the practical performances of LCO is typically limited by the instability at higher voltage and temperature. Dahéron and Lu have reported that HF is generated in the cell at high voltage, which is concomitant with the decomposition of electrolyte.[17,18] Various researchers have proposed the degradation mechanism of LCO at high voltage by HF, such as phase transition[19,20] or cobalt dissolution.[21] Until now, many research directions have been devised to improve the stability of LCO by preventing the degradation of LCO at the high voltage.[22,23] First, several prospective dopants have been investigated to enhance the stability of LCO.[24-26] Second, various surface coating agents have been suggested, such as SnO_2,[27] TiO_2,[28] ZrO_2,[29] and Al_2O_3 to protect the surface of LCO from the attack of HF.[30,31] Third, lithium-ion conducting materials have been coated on the surface of LCO as an artificial cathode-electrolyte interphase. Wang *et al.* and Zhou *et al*. coated lithium iron phosphate ($LiFePO_4$) and lithium phosphate (Li_3PO_4), respectively, to enhance the thermal stability.[32,33]

While stability of the LCO cathode has been magnificently enhanced with the above strategies, still fundamental studies are highly required to clarify the key mechanisms of degradation for further enhancement. In this study, we investigated the surface film formation on LCO cathode as a culprit of thermal degradation at high temperature. For this purpose, the LCO cathodes were cycled at different temperature of 25 and 60ºC for initial 5 cycles, followed by subsequent electrochemical characterizations of the impedance and rate capability. X-ray photoelectron spectroscopy (XPS) analysis detected excessive formation of cathode-electrolyte interphase at the high temperature, which was in line with the increase in the resistance from the electrochemical characterizations.

2. Experimental

2.1 Synthesis of $LiCoO_2$

Lithium cobalt oxide was prepared by solid-state synthesis. First, stoichiometric amounts of lithium carbonate (Li_2CO_3, Junsei Chemical Co., 99%) and cobalt oxide black (Co_3O_4, Junsei Chemical Co., >85%) were ball-milled for fine mixing and grinding. Subsequently, the precursors were transferred to box furnace for the heat treatment in two steps: (1) calcination at 800ºC for12 hours followed by natural cooling and grinding using the mortar and pestle and (2) sintering at 850ºC for 24 hours.

2.2 Electrochemical characterizations

In order for the electrochemical characterization of LCO, the composite electrodes were prepared using the synthesized LCO as the active material, carbon black (Super-P, Timcal Co.) as the conductive agent, polyvinylidene fluoride (PVDF, KF1100, Kureha Co.) as the binder, and N-methyl-2-pyrrolidone (NMP, Sigma Aldrich Co., 99.5%) as the solvent for the slurry. They were homogeneously

mixed so that the ratio of active material, conductive agent, and binder was 80:10:10 by mass. The slurry was coated on Al foil using doctor blade, and the coated electrodes were dried at 80ºC under vacuum for 2 hours. The dried electrodes were then pressed using roll presser and punched into discs with diameter of 11 mm. Active mass loading of the electrodes was controlled to *ca.* 1.0 mg cm^{-2}. 2032-type coin cells were assembled inside the glove box using the electrolyte solution of 1.0 M $LiPF_6$ in ethylene carbonate and ethyl methyl carbonate (EC:EMC = 3:7 w/w, Dongwha Electrolyte Co.). Lithium metal foil and porous polyethylene separator (Celgard Co.) were used as the counter electrode and separator, respectively. The coin cells were cycled using battery cycler (WBCS3000Le32, WonATech Co.). The C-rate was determined based on the theoretical capacity of 273.85 mAh g^{-1}. Electrochemical impedance spectroscopy (EIS) was measured at 3.0 V vs Li/Li^+ in the range of 200 kHz to 100 mHz using the rms amplitude of 5 mV (VMP3, Bio-Logic Co.). ZView (Scribner Co.) software was utilized for the complex nonlinear least squares (CNLS) fitting of the impedance data. Samples for X-ray photoelectron spectroscopy (XPS, AXIS SUPRA, Kratos Analytical Co.) was collected by disassembling the cells in the glove box, followed by thoroughly washing with dimethyl carbonate (DMC) solvent.

3. Results and Discussion

X-ray diffraction (XRD) patterns were analyzed using Pawley fitting with the space group of *R*-3*m* (hexagonal-166), which exhibits a layered structure with the unit cell parameters of 2.8160 (*a*) and 14.0626 Å (*c*) without any evidence of impurities (Fig. 1a). Intensity ratio of (003)/(104) was 1.272 (Fig. 1b and 1c), which is higher than 1.2, evidencing the absence of cation mixing that is detri-

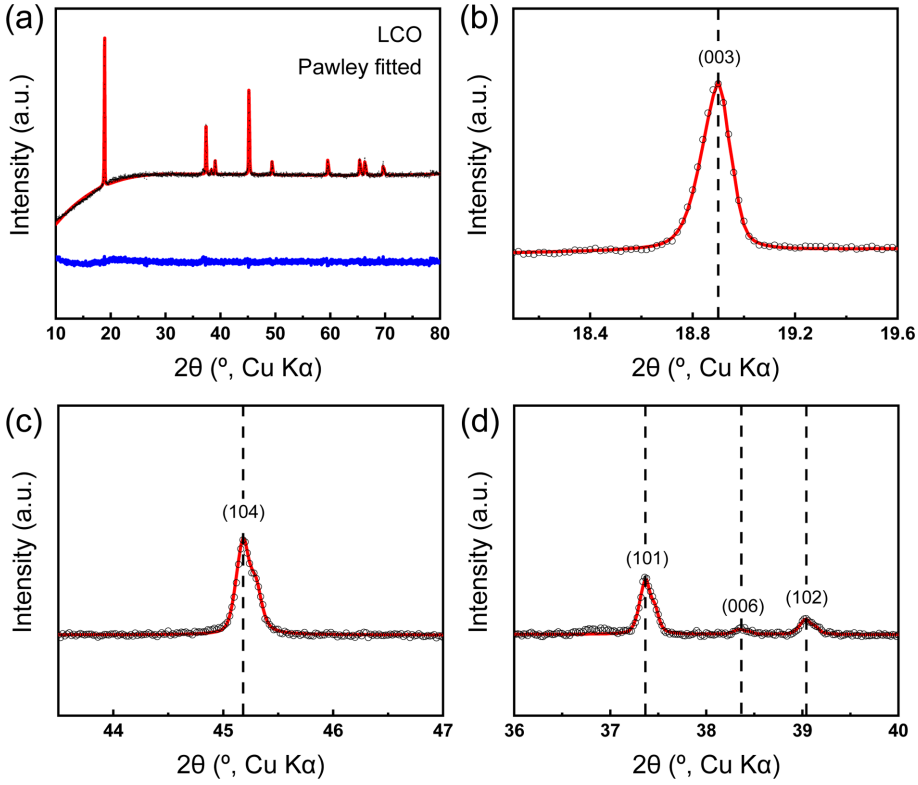

Fig. 1. X-ray diffraction patterns of the synthesized $LiCoO_2$. (a) Pawley fitting of the diffraction pattern and (b-d) zoomed-in views of the fitted patterns.

mental for the electrochemical performances.[34] Wang *et al*. mentioned that the clear splitting of the doublet of (006) and (102) peaks, as shown in Fig. 1d, indicates well-ordered layered structure of LCO.[35]

The LCO cells were operated at 25ºC (25-LCO) and 60ºC (60-LCO) for 5 cycles at 0.1C in the potential range of 3.0 ~ 4.3 V vs Li/Li^+. As shown in Fig. 2a and 2b, there were no magnificent differences between 25-LCO and 60-LCO in terms of the capacity, which was close to 150 mAh g^{-1} for the two cases during the 5 cycles. It is noteworthy that the voltage profiles of 60-LCO do not exhibit a plateau at 4.1 ~ 4.2 V vs Li/Li^+, which is related with a phase transition from hexagonal to monoclinic structure.[19] On the other hand, coulombic efficiency of 60-LCO was 93.9% and 98.2% for first and fifth cycles, respectively, whereas 25-LCO exhibited 97.7% and 99.7% for the first and fifth cycles, respectively (Fig. 2c). The lower coulombic efficiency of 60-LCO cell signifies more severe side reactions at the surface of the electrode. To confirm the accelerated degradation at high temperature, the 25-LCO and 60-LCO cells were cycled for 100 cycles at 25ºC and 60ºC, respectively. Capacity fading was more prominent at 60ºC compared to the operation at 25ºC (Fig. 2d); the capacity retention after 100 cycles was 90.34% and 59.52% at 25ºC and 60ºC, respectively.

The rate capability and impedance of 25-LCO and 60-LCO cells were compared at the equivalent temperature of 25ºC (Fig. 3 and 4). To exclude the influences from the anode side, the cells were disassembled after the initial 5 cycles at each temperature and the cells were reassembled using fresh Li metal anodes and electrolyte. Fu *et al*. pointed out that the gradual decrease of the capacity by the current density is mainly due to the polarization.[36] The 25-LCO and 60-LCO cells exhibit relatively similar discharge capacity of 147.5 and 140.3 mAh

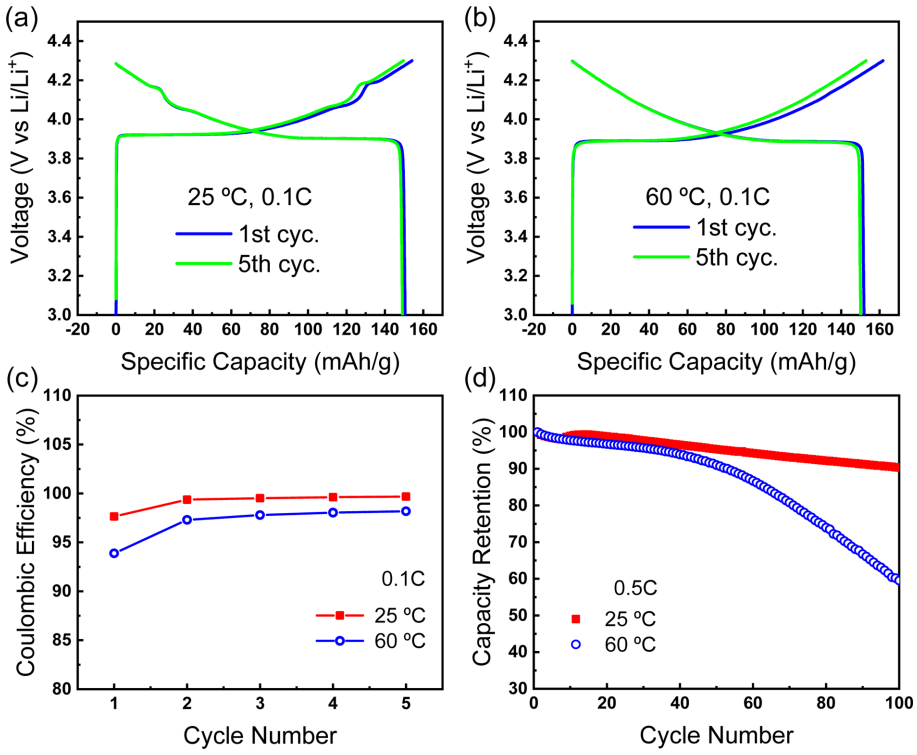

Fig. 2. Voltage profiles of LCO cells at (a) 25ºC and (b) 60ºC at 0.1C for 5 cycles. (c) Coulombic efficiency with respect to the cycle number during the initial cycling at each temperature. (d) Cycle performances of LCO cells at 25ºC and 60ºC under accelerate C-rate of 0.5C.

g^{-1}, respectively, at the lower C-rate of 0.1C, but the difference becomes more prominent as raising the C-rate. The capacity retention at 5C was 67.0% and 48.5% for 25-LCO and 60-LCO, respectively (Fig. 3b). The significantly lower capacity retention of 60-LCO cell was concomitant with its larger overpotential by 0.18 V at 5C (Fig. 3d).

In general, the charge transfer resistance is proportional to the over-potential.[37] EIS analysis represents significantly larger resistance for 60-LCO

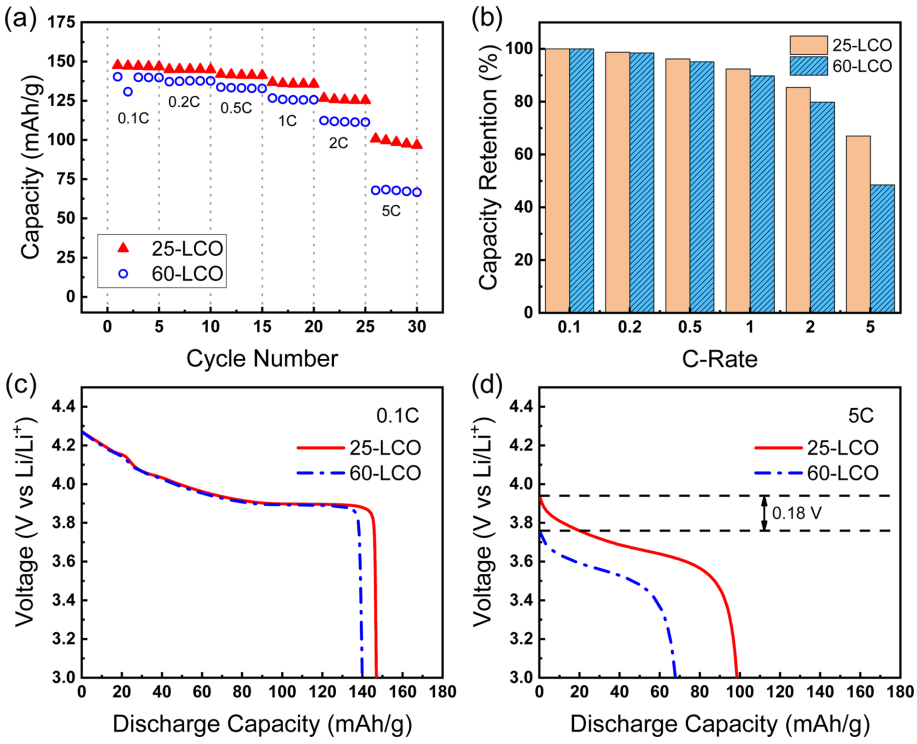

Fig. 3. Electrochemical characterization of 25-LCO and 60-LCO cells at room temperature after the initial cycling at 25 and 60°C, respectively. Comparison of (a) the rate capability and (b) the capacity retention at different C-rate. Overpotential in the discharge profiles were compared at (c) 0.1C and (d) 5C.

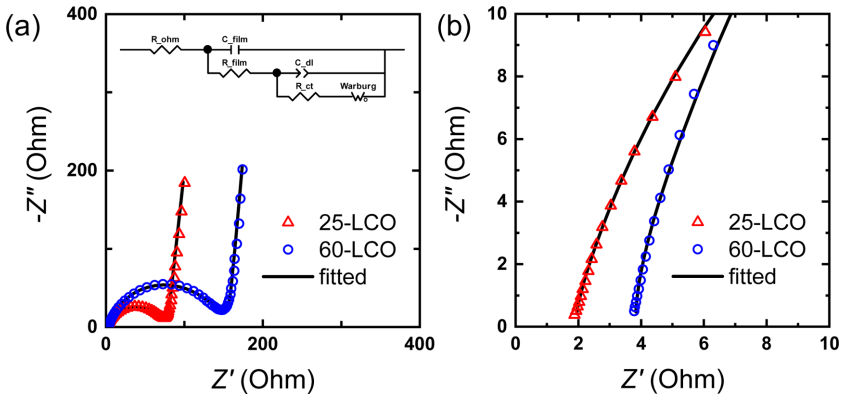

Fig. 4. EIS data compared with the fitted results. (a) Nyquist plots and (b) the zoomed-in view. The equivalent circuit for the fitting is in the inset of (a).

Table 1. Fitted parameters from the EIS analysis on 25-LCO and 60-LCO

	25-LCO	60-LCO
R_{ohm} (Ω)	1.91±0.01	3.82±0.01
C_{film} (μF)	1.84±0.05	1.67±0.02
R_{film} (Ω)	4.0±0.8	13±1
C_{dl} (CPE[1])	43±3	22±1
p (CPE)	0.681±0.008	0.717±0.007
R_{ct} (Ω)	67±1	125±2
W-R (Ω)	22±2	49±3
W-T (s)	0.040±0.005	0.088±0.006
W-p	0.467±0.001	0.473±0.001

[1]CPE stands for the constant phase element

compared with 25-LCO (Fig. 4 and Table 1). The diameter of the semicircle in the Nyquist plot of the impedance data may comprise surface film resistance (R_{film}) and charge transfer resistance (R_{ct}), while the ohmic resistance (R_{ohm}) is represented by the x-intercept at the highest frequency. And the spike at the lowest frequency represent solid-state diffusion of ions.[22] The fitted values of R_{film} + R_{ct} (*ca.* the diameter of the semicircle) was 71 Ω and 138 Ω for 25-LCO and 60-LCO, respectively (Fig. 4a), suggesting more sluggish charge transfer kinetics by the severer formation of surface film at 60ºC. It is noteworthy that the R_{ohm} of 60-LCO (3.82 Ω) is approximately two times larger than that of 25-LCO (1.91 Ω), implying sluggish migration of Li^+ ions by the formation of surface film. Also, the larger values of diffusion resistance (W-R) and diffusion time constant (W-T) of 60-LCO signify the higher overpotential of Li^+ diffusion compared to 25-LCO. Those overall increase in the resistance is in line with the deteriorated rate capability of 60-LCO cell compared with 25-LCO cell.

XPS analysis of 25-LCO and 60-LCO revealed the different composition on the surface of the cathodes by the operational temperature for 5 cycles (Fig. 5 and 6). Chemical compositions from XPS analysis are summarized in Table 2. Most stark differences were observed in O 1s region as shown in

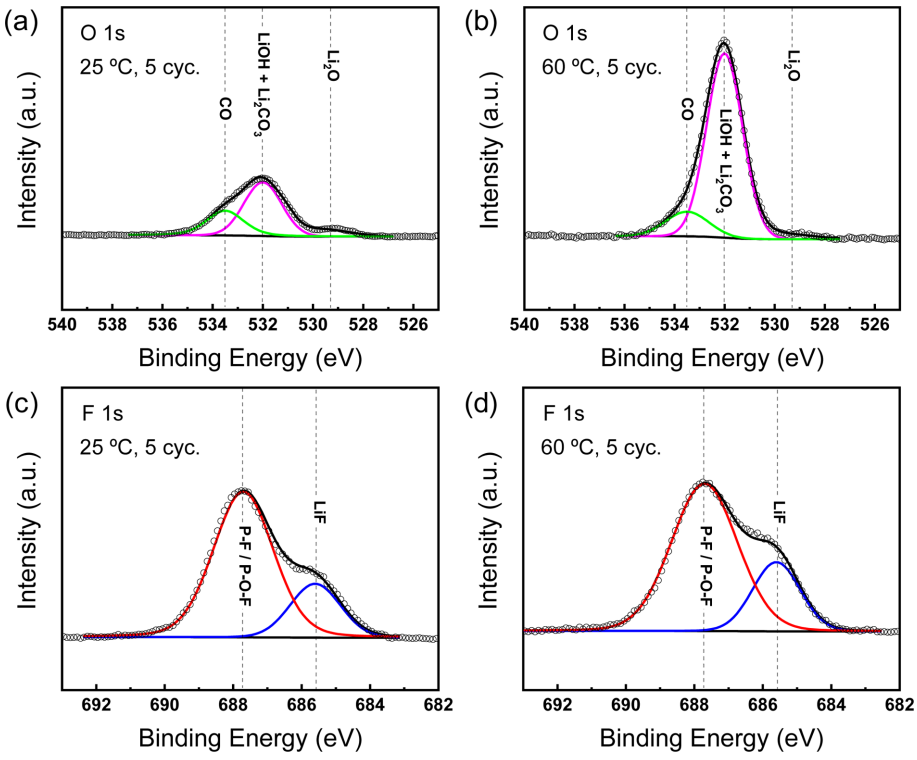

Fig. 5. Results of XPS analysis: O 1s peaks of (a) 25-LCO and (b) 60-LCO, and F 1s peaks of (c) 25-LCO and (d) 60-LCO.

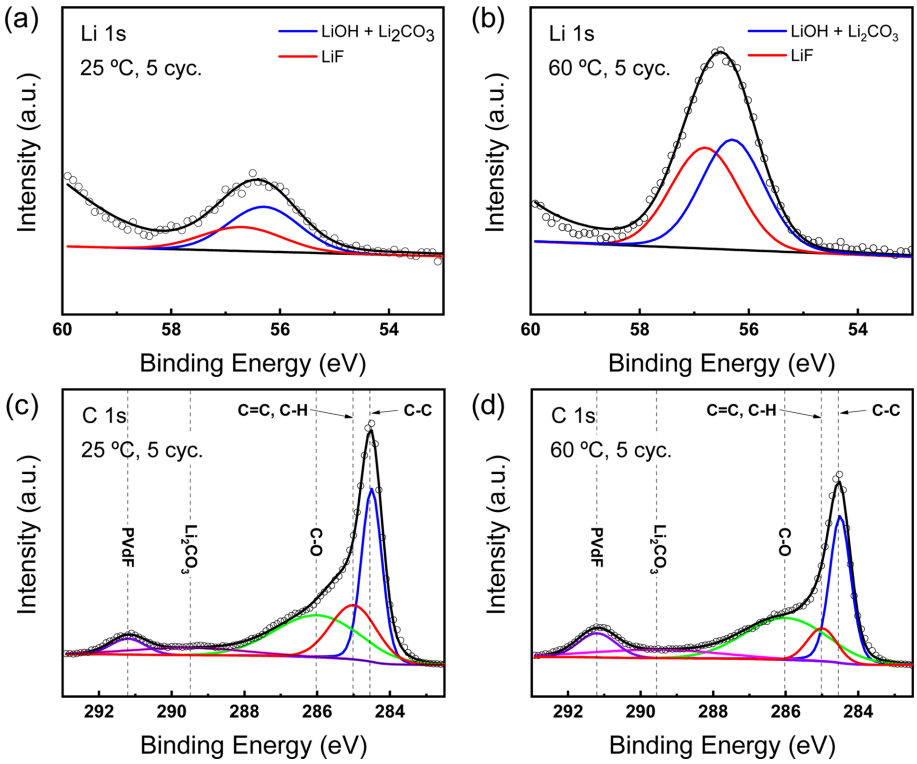

Fig. 6. Results of XPS analysis: Li 1s peaks of (a) 25-LCO and (b) 60-LCO, and C 1s peaks of (c) 25-LCO and (d) 60-LCO.

Table 2. Percentage (%) of chemical compositions in 25-LCO and 60-LCO based on the XPS spectra

		25-LCO	60-LCO
O 1s	$LiOH / Li_2CO_3$	65.0	90.0
	C-O	35.0	10.0
F 1s	LiF	22.6	24.8
	P-O-F	77.4	75.2
Li 1s	$LiOH / Li_2CO_3$	62.4	51.6
	LiF	37.6	48.4
C 1s	C-C	33.5	34.5
	C=C / C-H	22.4	9.9
	C-O	31.9	35.2
	Li_2CO_3	7.3	11.0
	PVdF	4.9	9.4

Fig. 5a and 5b. The 529.3, 532.0, and 533.5 eV peaks correspond to Li_2O, $LiOH/Li_2CO_3$, C-O group, respectively,[18] which are representative components of CEI film.[38] Among them, the peak at 532.0 eV for LiOH or Li_2CO_3 components was especially intense for 60-LCO compared to 25-LCO, suggesting that the cathode surface is covered with CEI with richer proportion of LiOH or Li_2CO_3 at 60ºC. Regarding the F 1s region, the two peaks at 685.6 and 687.7 eV are attributed to Li-F and P-F/P-O-F, respectively.[39,40] Li-F and P-O-F are the well-known product from the decomposition of electrolytes. [41] Peak intensity at 685.6 eV of 60-LCO was slightly larger than that of 25-LCO, while peak intensities at 687.7 eV were almost equivalent for both samples (Fig. 5c and 5d); this suggests the accelerated formation of LiF at 60ºC. In accordance with the O 1s and F 1s results, the Li 1s peak at 56.3 eV for $LiOH/Li_2CO_3$ or LiF was more intense for 60-LCO compared to that of 25-LCO (Fig. 6a and 6b). On the other hand, C 1s peaks provided more clues to discern which components are dominant in the CEI film (Fig. 6c and 6d). The C 1s peaks at 284.5, 285.0, 286.0, 289.5,

293.1 eV correspond to C-C, C=C/C-H, C-O, Li_2CO_3, and PVdF, respectively. The Li_2CO_3 peak at 289.5 eV was not significant for both 25-LCO and 60-LCO, suggesting that Li_2CO_3 can be excluded from the dominant components in the CEI film of 60-LCO. The C-C and C=C/C-H peaks of 60-LCO was less intense compared to 25-LCO, while the intensity of C-O peaks were similar for both samples; this observation suggests that the conductive agent was more severely covered by CEI film for 60-LCO. To summarize, it is highly probable that the thermally accelerated formation of CEI film is associated with LiOH and LiF as the dominant components, which lead to the increase in the resistance that limits the electrochemical performances of cells, owing to their insulating property. Such accelerated formation of Li species also signifies the continual loss of Li^+ ions from the $LiPF_6$ electrolyte or LCO cathode, which starves the electrolyte or reduces the utilizable capacity of LIBs at higher temperature.

4. Conclusions

Decomposition of electrolytes and cathode was accelerated at high temperature, resulting in the higher overall impedance and the lower rate capability even by the initial 5 cycles at 60ºC. In particular, initial cycling at 60°C exhibited more prominent increase in Li species such as LiOH and LiF compounds on the surface of the electrodes, identifying the adverse effects of the insulating film on the electrochemical performances of LIB cells. This finding signifies a culprit of thermal instability of LCO cathodes, and points to the necessity of mitigating the thermo-electrochemical decomposition by introducing advanced electrolyte solutions, additives, and artificial interphase.

Acknowledgement

This work was supported by a 2-Year Research Grant of Pusan National University.

References

1. Y. Nishi, 'Lithium ion secondary batteries; past 10 years and the future', *J. Power Sources*, **100**, 101 (2001).
2. J.-Y. Hwang, S.-T. Myung and Y.-K. Sun, 'Sodium-ion batteries: present and future', *Chem. Soc. Rev.*, **46**, 3529 (2017).
3. J. Zheng, P. Yan, L. Estevez, C. Wang and J.-G. Zhang, 'Effect of calcination temperature on the electrochemical properties of nickel-rich $LiNi_{0.76}Mn_{0.14}Co_{0.10}O_2$ cathodes for lithium-ion batteries', *Nano Energy*, **49**, 538 (2018).
4. W. Cho, Y. J. Lim, S.-M. Lee, J. H. Kim, J.-H. Song, J.-S. Yu, Y.-J. Kim and M.-S. Park, 'Facile Mn surface doping of Ni-rich layered cathode materials for lithium ion batteries', *ACS Appl. Mater. Interfaces*, **10**, 38915 (2018).
5. L. Zhu, T.-F. Yan, D. Jia, Y. Wang, Q. Wu, H.-T. Gu, Y.-M. Wu and W.-P. Tang, '$LiFePO_4$-Coated $LiNi_{0.5}Co_{0.2}Mn_{0.3}O_2$ Cathode Materials with Improved High Voltage Electrochemical Performance and Enhanced Safety for Lithium Ion Pouch Cells', *J. Electrochem. Soc.*, **166**, A5437 (2019).
6. Z. Wu, Y. Wang, X. Liu, C. Lv, Y. Li, D. Wei and Z. Liu, 'Carbon Nanomaterial Based Flexible Batteries for Wearable Electronics', *Adv. Mater.*, **31**, 1800716 (2019).
7. Y. Park, S. H. Shin, H. Hwang, S. M. Lee, S. P. Kim, H. C. Choi and Y. M. Jung, 'Investigation of solid electrolyte interface (SEI) film on $LiCoO_2$ cathode in fluoroethylene carbonate (FEC)-containing electrolyte by 2D correlation X-ray photoelectron spectroscopy (XPS)', *J. Mol. Struct.*, **1069**, 157 (2014).
8. F. Zheng, M. Kotobuki, S. Song, M. O. Lai and L. Lu, 'Review on solid electrolytes for all-solid-state lithium-ion batteries', *J. Power Sources*, **389**, 198 (2018).
9. J. B. Goodenough and Y. Kim, 'Challenges for rechargeable Li batteries', *Chem. Mater.*, **22**, 587 (2009).
10. V. Etacheri, R. Marom, R. Elazari, G. Salitra and D. Aurbach, 'Challenges in the development of advanced Li-ion batteries: a review', *Energy Environ. Sci.*, **4**, 3243 (2011).
11. D. H. Doughty and E. P. Roth, 'A general discussion of Li ion battery safety', *Electrochem. Soc. Interface*, **21**, 37 (2012).
12. L. Lu, X. Han, J. Li, J. Hua and M. Ouyang, 'A review on the key issues for lithium-ion battery management in electric vehicles', *J. Power Sources*, **226**, 272 (2013).
13. P. Balakrishnan, R. Ramesh and T. P. Kumar, 'Safety mechanisms in lithium-ion batteries', *J. Power Sources*, *155*, 401 (2006).
14. A. Jansen, A. Kahaian, K. Kepler, P. Nelson, K. Amine, D. Dees, D. Vissers and M. Thackeray, 'Development of a high-power lithium-ion battery', *J. Power Sources*, **81**, 902 (1999).
15. K. Liu, Y. Liu, D. Lin, A. Pei and Y. Cui, 'Materials for lithium-ion battery safety', *Sci. Adv.*, **4**, eaas9820 (2018).
16. K. Mizushima, P. Jones, P. Wiseman and J. B. Goodenough, 'Li_xCoO_2 ($0<x<1$): A new cathode material for batteries of high energy density', *Mater. Res. Bull.*, **15**, 783 (1980).
17. L. Dahéron, R. Dedryvere, H. Martinez, D. Flahaut, M. Ménétrier, C. Delmas and D. Gonbeau, 'Possible Explanation for the Efficiency of Al-Based Coatings on

$LiCoO_2$: Surface Properties of $LiCo_{1-x}Al_xO_2$ Solid Solution', *Chem. Mater.*, **21**, 5607 (2009).
18. Y.-C. Lu, A. N. Mansour, N. Yabuuchi and Y. Shao-Horn, 'Probing the origin of enhanced stability of "$AlPO_4$" nanoparticle coated $LiCoO_2$ during cycling to high voltages: combined XRD and XPS studies', *Chem. Mater.*, **21**, 4408 (2009).
19. J. Cho, Y. J. Kim and B. Park, '$LiCoO_2$ cathode material that does not show a phase transition from hexagonal to monoclinic phase', *J. Electrochem. Soc.*, **148**, A1110 (2001).
20. J. N. Reimers and J. Dahn, 'Electrochemical and in situ X-ray diffraction studies of lithium intercalation in Li_xCoO_2', *J. Electrochem. Soc.*, **139**, 2091 (1992).
21. G. Amatucci, J. Tarascon and L. Klein, 'CoO_2, the end member of the Li_xCoO_2 solid solution', *J. Electrochem. Soc.*, **143**, 1114 (1996).
22. J.-N. Zhang, Q. Li, Y. Wang, J. Zheng, X. Yu and H. Li, 'Dynamic evolution of cathode electrolyte interphase (CEI) on high voltage $LiCoO_2$ cathode and its interaction with Li anode', *Energy Storage Materials*, **14**, 1 (2018).
23. A. Yano, M. Shikano, A. Ueda, H. Sakaebe and Z. Ogumi, '$LiCoO_2$ degradation behavior in the high-voltage phase transition region and improved reversibility with surface coating', *J. Electrochem. Soc.*, **164**, A6116 (2017).
24. S.-T. Myung, N. Kumagai, S. Komaba and H.-T. Chung, 'Effects of Al doping on the microstructure of $LiCoO_2$ cathode materials', *Solid State Ionics*, **139**, 47 (2001).
25. M. Zou, M. Yoshio, S. Gopukumar and J.-i. Yamaki, 'Synthesis of high-voltage (4.5 V) cycling doped $LiCoO_2$ for use in lithium rechargeable cells', *Chem. Mater.*, **15**, 4699 (2003).
26. A. Liu, J. Li, R. Shunmugasundaram and J. Dahn, 'Synthesis of Mg and Mn Doped $LiCoO_2$ and Effects on High Voltage Cycling', *J. Electrochem. Soc.*, **164**, A1655 (2017).
27. C. Hudaya, J. H. Park, J. K. Lee and W. Choi, 'SnO_2-coated $LiCoO_2$ cathode material for high-voltage applications in lithium-ion batteries', *Solid State Ionics*, **256**, 89 (2014).
28. A. Zhou, Y. Lu, Q. Wang, J. Xu, W. Wang, X. Dai and J. Li, 'Sputtering TiO_2 on $LiCoO_2$ composite electrodes as a simple and effective coating to enhance high-voltage cathode performance', *J. Power Sources*, **346**, 24 (2017).
29. B. Hwang, C. Chen, M. Cheng, R. Santhanam and K. Ragavendran, 'Mechanism study of enhanced electrochemical performance of ZrO_2-coated $LiCoO_2$ in high voltage region', *J. Power Sources*, **195**, 4255 (2010).
30. S. Oh, J. K. Lee, D. Byun, W. I. Cho and B. W. Cho, 'Effect of Al_2O_3 coating on electrochemical performance of $LiCoO_2$ as cathode materials for secondary lithium batteries', *J. Power Sources*, **132**, 249 (2004).
31. Y.-H. Chang and S. Y. Choi, 'Analyses on the Physical and Electrochemical Properties of Al_2O_3 Coated $LiCoO_2$', *J. Korean Electrochem. Soc.*, **10**, 184 (2007).
32. H. Wang, W.-D. Zhang, L.-Y. Zhu and M.-C. Chen, 'Effect of $LiFePO_4$ coating on electrochemical performance of $LiCoO_2$ at high temperature', *Solid State Ionics*, **178**, 131 (2007).
33. A. Zhou, J. Xu, X. Dai, B. Yang, Y. Lu, L. Wang, C. Fan and J. Li, 'Improved high-voltage and high-temperature electrochemical performances of $LiCoO_2$ cathode by electrode sputter-coating with Li_3PO_4', *J. Power Sources*, **322**, 10 (2016).
34. X. Zhu, K. Shang, X. Jiang, X. Ai, H. Yang and Y. Cao, 'Enhanced electrochemical performance of Mg-doped $LiCoO_2$ synthesized by a polymer-pyrolysis method', *Ceram. Int.*, **40**, 11245 (2014).
35. Z. Wang, Z. Wang, H. Guo, W. Peng, X. Li, G. Yan and J. Wang, 'Mg doping and zirconium oxyfluoride coating co-modification to enhance the high-voltage performance of $LiCoO_2$ for lithium ion battery', *J. Alloys Compd.*, **621**, 212 (2015).
36. J. Fu, D. Mu, B. Wu, J. Bi, H. Cui, H. Yang, H. Wu and F. Wu, 'Electrochemical properties of the $LiNi_{0.6}Co_{0.2}Mn_{0.2}O_2$ cathode material modified by lithium tungstate under high voltage', *ACS Appl. Mater. Interfaces*, **10**, 19704 (2018).
37. P. Elumalai, H. Vasan and N. Munichandraiah, 'A note on overpotential dependence of AC impedance data', *J. Solid State Electrochem.*, **3**, 470 (1999).
38. J. Kim, J. Lee, H. Ma, H. Y. Jeong, H. Cha, H. Lee, Y. Yoo, M. Park and J. Cho, 'Controllable Solid Electrolyte Interphase in Nickel-Rich Cathodes by an Electrochemical Rearrangement for Stable Lithium-Ion Batteries', *Adv. Mater.*, **30**, 1704309 (2018).
39. Z. W. Lebens-Higgins, S. Sallis, N. V. Faenza, F. Badway, N. Pereira, D. M. Halat, M. Wahila, C. Schlueter, T.-L. Lee and W. Yang, 'Evolution of the Electrode–Electrolyte Interface of $LiNi_{0.8}Co_{0.15}Al_{0.05}O_2$ Electrodes Due to Electrochemical and Thermal Stress', *Chem. Mater.*, **30**, 958 (2018).
40. S. Verdier, L. El Ouatani, R. Dedryvere, F. Bonhomme, P. Biensan and D. Gonbeau, 'XPS study on Al_2O_3-and $AlPO_4$-coated $LiCoO_2$ cathode material for high-capacity Li ion batteries', *J. Electrochem. Soc.*, **154**, A1088 (2007).
41. J. Chen, L. Zhu, D. Jia, X. Jiang, Y. Wu, Q. Hao, X. Xia, Y. Ouyang, L. Peng and W. Tang, '$LiNi_{0.8}Co_{0.15}Al_{0.05}O_2$ cathodes exhibiting improved capacity retention and thermal stability due to a lithium iron phosphate coating', *Electrochim. Acta*, **312**, 179 (2019).